Comparative Evaluation of Isolated dc-dc Converters for Low Power Applications

Mohammadreza Azizi[1,2], Oleksandr Husev[1,2], Dmitri Vinnikov[2], Oleksandr Veligorskyi[1]
[1]Department of Radiotechnic and Embedded Systems, Chernihiv Polytechnic National University, Chernihiv, Ukraine
[2]Department of Electrical Power Engineering and Mechatronics, Tallinn, Estonia
Azizi.malayeru@gmail.com

***Abstract*— Isolated dc-dc converters are particularly important for utilizing renewable energy. These converters are used for direct connection to the dc microgrid or as voltage boosters for on/off-grid ac applications. This article examines and evaluates five popular types of isolated dc-dc converters for low-power applications. In this study, by examining the performance of converters, the general equations governing these converters have been extracted. The converter components are then designed for a low-power application. Using simulations in Simulink/MATLAB, these converters have been evaluated and compared from different perspectives.**

Keywords— Isolated dc-dc converters, Component design, Flyback, Forward, Push-pull, Full-bridge.

I. Introduction

Today, power electronic converters are used in almost all home and industrial appliances. Research into the development and improvement of these converters is the subject of many studies. Due to environmental concerns and the need to use more green energy resources, the use of these converters as an intermediary between renewable sources and the grid is growing notably. Since most renewables, e.g. solar are dc, existing structures use a dc-dc boost converter and then an inverter. Although the use of single-stage inverters with the ability to increase/decrease voltage has been considered by researchers in recent years, they still face challenges [1]. The use of dc-dc converters in dc or hybrid microgrids is also a topic of the day. Due to the dc nature of renewable resources and many dc loads, the use of dc-dc converters in hybrid microgrids is conceivable in the near future [2].

Among the various dc-dc converters, isolated converters have higher reliability. A high-frequency transformer with low weight and volume in its structure increases the reliability of the converter by creating isolation and can also increase the gain of the converter through the turn ratio. The flyback converter is a widely used structure and is usually used in the low power range [3],[4]. Many researchers have tried to improve the performance of this converter by providing derivatives of it [5],[6]. Snubber circuit design or switching improvements are among these studies [7],[8]. In [8],[9], this converter with two differential outputs has been used as a single-stage inverter, while in [7], is used as the dc-dc booster step in a solar inverter. Another known dc-dc isolated structure is the forward converter. This converter is reviewed in references[10],[11]. The use of a third winding to reset the circuit and instantaneous conversion of energy through the operation of the transformer are some of the features of this converter. Researchers have also proposed derivative structures to improve this converter. In dual-switch structure, the use of two switches reduces the voltage across the switch, and there are two diodes on the primary side instead of the third winding to reset the circuit [10]. Other commonly used dc-dc isolated converters include push-pull and full-bridge converters [12],[13]. The use of a three-taps transformer and the operation of each of the two switches in each half-cycle are characteristic of the push-pull converter. As in each half-cycle, one of the switches is conducting and the voltage source is empowering, the utilization rate of the voltage source will be higher.

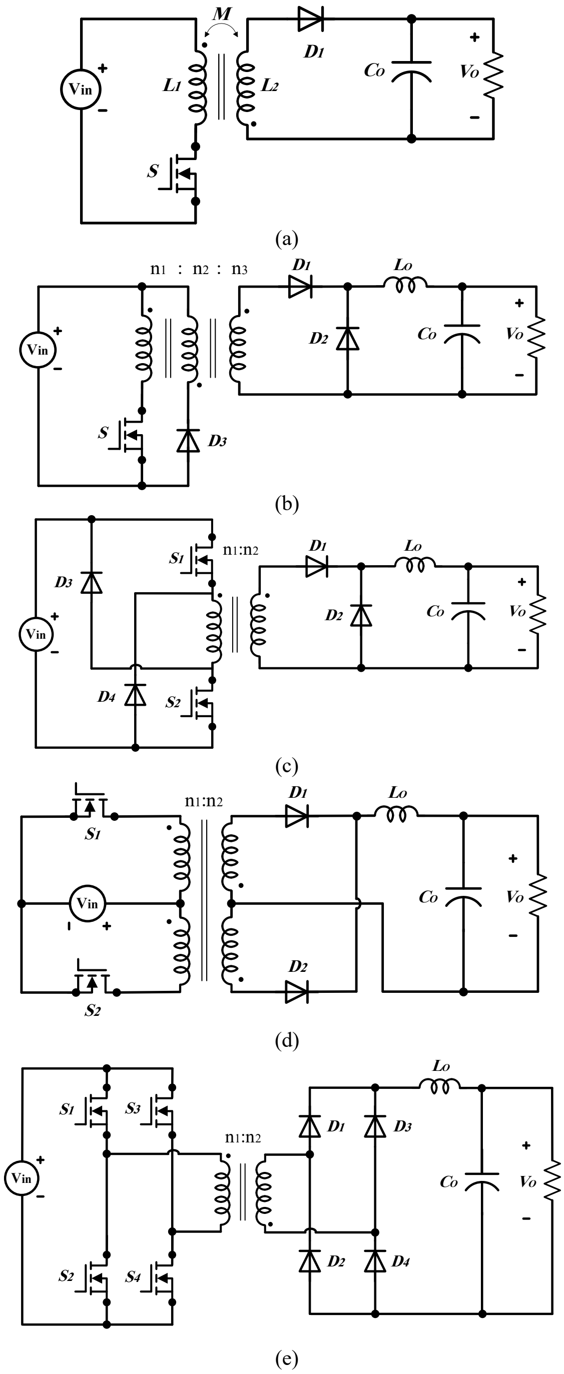

Fig. 1. Five well-known isolated dc-dc converters. a) Flyback b) Forward c) Dual-Switch Forward d) Push-Pull e) Full-bridge

The full-bridge converter has also been welcomed as a well-known and widely used structure in all power ranges or as a bidirectional converter in many applications [14]. With the development of power electronic converters, these types of isolated converters are still widely used in many low-power applications. Several studies have compared and analyzed some of these converters [15]-[17]. In this study, the aim is to evaluate and compare the above five converters in a high step-up low-power application for dc grid connection. In this study, first, the general relationships of these converters are extracted, then the design and comparison of passive elements, selection of semiconductor components and their losses are investigated. Finally, the results are discussed.

II. DESIGN OF ISOLATED CONVERTERS

Fig. 1 shows the five well-known isolated structures including flyback, forward, dual-switch forward (DS-forward), push-pull, and full-bridge converter. The use of high-frequency magnetics in these structures is for primary and secondary isolation, which is associated with increasing gain and the reliability of the converter. To design the elements of these converters, the optimal values of the elements should be calculated by analyzing the performance in different operating modes and extracting the relationships governing them. In this section, by examining the flyback converter, its elements will be designed. Similarly, for the other converters considered in this study, general equations will be extracted and summarized in a table. Then, based on equations, their components will be designed.

A. Flyback converter design

Fig. 1a shows the flyback converter. This single-switch converter has been used in many low-power applications and offers significant advantages. This structure works on coupling inductors and also provides insulation between input and output. Other features include the possibility of using multiple outputs with different voltage levels and, the presence of an air gap in the core structure of the windings to absorb energy and prevent the core from saturating. In this converter, by turning on the switch, the current passes through the primary side of the transformer and the magnetic inductance will be charged linearly. The energy stored in this inductance begins to discharge from the diode path by turning off the switch. Then the output capacitor is charged and finally the power will be delivered to the output. Taking into account the magnetic inductance in the equivalent circuit, Fig. 2a and 2b show this converter in both switched-on and off modes.

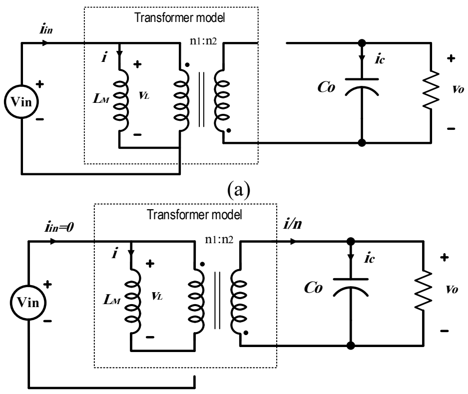

Fig. 2. Equivalent circuit of the flyback converter. a) When the switch is on. b) When the switch is off

Ignoring small signal fluctuations and applying Kirchhoff's Voltage and Current Laws (KVL & KCL) and applying the inductor voltage balance and the output capacitor current balance, the following equations will obtain:

$$DV_{in} + D'\left(\frac{-V_o}{n}\right) = 0 \;\Rightarrow\; \frac{V_o}{V_{in}} = \frac{D}{D'}n = \frac{D}{1-D}n, \tag{1}$$

$$D\left(\frac{-V_o}{R}\right) + D'\left(\frac{I}{n} - \frac{V_o}{R}\right) = 0 \Rightarrow I = \frac{nV_o}{D'R} = \frac{nV_o}{(1-D)R}, \tag{2}$$

$$I_{in} = DI. \tag{3}$$

Where D corresponds to the duration of the switch being on. To calculate the magnetizing inductance, the inductor voltage relation in the first interval will be as:

$$L_M \frac{\Delta i}{DT} = V_{in} \;\Rightarrow\; L_M = \frac{V_{in} D}{2 f_s \Delta I_M}. \tag{4}$$

Considering the ripple factor and the relationship between efficiency and power as below,

$$K = \frac{\Delta I_M}{I_M} \quad , \quad P_{in} = \frac{P_o}{\eta}, \tag{5}$$

And replacing equations (3) and (5) in equation (4), the magnetizing inductance will be:

$$L_M = \frac{DV_{in}}{2K_{L_M} f_s I_M}. \tag{6}$$

Also,

$$I_M = \frac{n_2 V_o}{n_1 (1-D) R} = \frac{n_2 P_o}{n_1 (1-D) V_o}. \tag{7}$$

Replacing (7) in (6) and considering the gain equation:

$$L_M = \frac{D^2 V_{in}^2}{2K_{L_M} f_s P_o}. \tag{8}$$

To design the output capacitor, in the first interval:

$$i_c = \frac{V_o}{R} \;\Rightarrow\; C = \frac{V_o D}{R f_s \Delta V_o}. \tag{9}$$

Considering the ripple factor K_c, the maximum required capacitor is:

$$C_{\max} = \frac{D_{\max}}{R f_s K_C} \quad , \quad K_C = \frac{\Delta V_o}{V_o}. \tag{10}$$

According to the gain relationship, the turn ratio of the transformer and the converter's duty cycle can also be expressed by the following equation,

$$n = \frac{n_2}{n_1} = \frac{(1-D_{\max})V_o}{V_{in-\max} D_{\max}} \quad , \quad D = \frac{V_o}{V_o + nV_{in}}. \tag{11}$$

When the switch is off, the maximum voltage across the switch is specified as below:

$$V_{switch} = V_{in} - V_L \Rightarrow V_L = \frac{-V_o}{n}. \tag{12}$$

Replacing V_o from the gain equation,

$$V_{S-\max} = V_{in-\max} + \frac{D_{max} V_{in-\min}}{1 - D_{max}}. \tag{13}$$

Also, for maximum current passing through the switch while the switch is on,

$$I_{S-\max} = \frac{P_o}{\eta D_{\max} V_{in-\min}} + \frac{D_{\max} V_{in-\min}}{2 f_s L_M}. \quad (14)$$

In this equation, the first sentence is the average input current and the second sentence is the maximum inductor current ripple. By applying a KVL, the maximum voltage across the secondary side diode also can be written as follow:

$$V_{D1-\max} = \frac{n_2}{n_1} V_{in} + V_o = \frac{V_o}{D} = \frac{n_2}{n_1} \frac{V_{in}}{1-D}. \quad (15)$$

And for current passing through the diode:

$$I_{D1-\max} = \frac{V_o}{(1-D_{\max}) R}. \quad (16)$$

It should be noted that while the switch is off, the diode will conduct energy corresponding to 1-D time.

In the same way, these equations are obtained for other converters. Table I summarize the required specifications of the five mentioned converters. Since DS-forward, push-pull, and full-bridge also work based on buck converter, they have similar equations to the forward converter. Of course, it should be noted that, unlike flyback and forwards converters, the duty cycle of push-pull and full-bridge is in range of zero to one.

III. Methodology of Evaluation

In this section, the purpose is to simulate and compare the above converters. Table II lists the specifications of the converter required for evaluation. Due to the gain relationship of the flyback converter based on the buck-boost converter and its duty cycle range, the turn ratio of the coupled inductors in this converter is considered to be 20. The other converters in this study operate based on buck converters. For the stable operation of the forward converters, the duty cycle must be less than 0.5. Due to the gain relationship in these converters, to produce an output voltage of 350 V with an input voltage of 24-36 V, a higher transformer turn ratio is required. To simulate these two types of forward converters in these simulations, the transformer turn ratio is set to 38. For the two converters of push-pull and full-bridge, the duty cycle is between zero and one. Therefore, in push-pull and full-bridge converters, like flyback, the turn ratio is considered to be 20. In Table 2, the K coefficient is considered for all converters except flyback. The flyback converter has a continuous magnetizing current and coefficient K in the flyback converter is the ratio of the magnetizing current ripple to the dc value of this current. While for other converters, this coefficient is the ratio of the maximum magnetizing current to the input current difference. This coefficient is assumed to be 0.05 for the flyback converter in the simulation. In the following sections, these converters are examined and compared from different aspects.

A. Passive elements design

In this section, according to the extracted relationships for magnetizing inductance, output inductance and output capacitor, the required values of elements in the input voltage range of 24 to 58 V are compared. Due to the converter gain equations, the converter operation is possible at an input voltage higher than 36 V. (58 V, is the case that there are four series batteries in the input, under charging). Fig. 3 shows the magnetizing inductance curve for the five desired converters. As it turns out, the push-pull converter requires the highest magnetic inductance. The lowest value belongs to the flyback converter which is due to the continuous magnetizing current in this converter. The magnetizing inductance curve for other converters can also be seen in the figure based on their equation in the table and the ripple coefficient considered.

A comparison between the output inductance values for the forwards, push-pull and full-bridge converters is shown in Fig. 4. As the input voltage increases, the required duty cycle will decrease and as shown, the inductance required for these converters increases. As it is clear, the forward converters require more inductance at the output. This is due to the lower

TABLE I. Converter design equations

	Flyback	Forward	DS-forward	Push-pull	Full-bridge
L_M	$\frac{D^2 V_{in}^2}{2K f_s P_o}$	$\frac{2(1-2K) f_s L_o D^2 V_{in}^2}{2K f_s^2 L_o P_o + K f_s (1-D) V_o^2}$	$\frac{(1-2K) f_s L_o D^2 V_{in}^2}{2K f_s^2 L_o P_o + K f_s (1-D) V_o^2}$	$\frac{2(1-K) f_s L_o D^2 V_{in}^2}{2K f_s^2 L_o P_o + K f_s (1-D) V_o^2}$	$\frac{(1-2K_1) f_s L_o D^2 V_{in}^2}{2K f_s^2 L_o P_o + K f_s (1-D) V_o^2}$
L_O	-	$\frac{(1-D_{\min}) V_o^2}{2K_{Lo} f_s P_o}$	$\frac{(1-D_{\min}) V_o^2}{2K_{Lo} f_s P_o}$	$\frac{(1-D_{\min}) V_o^2}{2K_{Lo} f_s P_o}$	$\frac{(1-D_{\min}) V_o^2}{2K_{Lo} f_s P_o}$
C_O	$\frac{D_{\max}}{R f_s K_C}$	$\frac{1-D_{\min}}{8K_C f_s^2 L_o}$	$\frac{1-D_{\min}}{8K_C f_s^2 L_o}$	$\frac{D_{\max}}{8K_C f_s^2 L_o}$	$\frac{D_{\max}}{8K_C f_s^2 L_o}$
$V_{S\text{-max}}$	$V_{in-\max} + \frac{D_{max} V_{in-\min}}{1-D_{max}}$	$(1+n_1/n_2) V_{in}$	V_{in}	$2V_{in}$	V_{in}
$I_{S\text{-max}}$	$\frac{P_o}{\eta D V_{in}} + \Delta I_{L_M}$	$\frac{P_o}{\eta D V_{in}} + \Delta I_{L_M} + \Delta I_{L_o}$	$\frac{P_o}{\eta D V_{in}} + \Delta I_{L_M} + \Delta I_{L_o}$	$\frac{P_o}{\eta D V_{in}} + \Delta I_{L_M} + \Delta I_{L_o}$	$\frac{P_o}{\eta D V_{in}} + \Delta I_{L_M} + \Delta I_{L_o}$
$V_{D1\text{-max}}$	$\frac{n_2}{n_1} \frac{V_{in}}{1-D}$	$\frac{n_2}{n_1} V_{in}$	$\frac{n_2}{n_1} V_{in}$	$2\frac{n_2}{n_1} V_{in}$	$\frac{n_2}{n_1} V_{in}$
$I_{D1\text{-max}}$	$\frac{V_o}{(1-D_{\max}) R}$	$\frac{(1-D) V_o}{2 f_s L_o} + \frac{V_o}{R}$	$\frac{(1-D) V_o}{2 f_s L_o} + \frac{V_o}{R}$	$\frac{(1-D) V_o}{8 f_s L_o D} + \frac{V_o}{R}$	$\frac{(1-D) V_o}{8 f_s L_o D} + \frac{V_o}{R}$
n_2/n_1	$\frac{(1-D_{\max}) V_o}{V_{in-\max} D_{\max}}$	$\frac{n_3}{n_1} = \frac{V_o}{D V_{in}}$	$\frac{V_o}{D V_g}$	$\frac{V_o}{D V_g}$	$\frac{V_o}{D V_g}$
D	$\frac{V_o}{V_0 + (n_2/n_1) V_{in}}$	$\frac{n_1}{n_3} \frac{V_o}{V_{in}}$	$\frac{n_1}{n_2} \frac{V_o}{V_{in}}$	$\frac{n_1}{n_2} \frac{V_o}{V_{in}}$	$\frac{n_1}{n_2} \frac{V_o}{V_{in}}$

duty cycle compared to the push-pull and full-bridge converters. It should also be noted that the high value of the output inductance is due to the low output current. Finally, Fig. 5 compares the required output capacitors which are drawn using the capacitor output relationships for these converters. As can be seen, the flyback converter requires a larger capacitor at the output. As the input voltage increases, the value of the capacitor for the flyback, push-pull and full-bridge converters decreases and is almost constant for the forward converters.

TABLE II. GENERAL SPECIFICATIONS OF SIMULATED CONVERTERS

Specifications	Value
Input voltage (V_g)	24 V to 36 V
Output voltage (V)	350 V
Output power	200 W
Ripple factor of I_{LM} (K)	0.005
Ripple factor of I_{Lo} (K_{Lo})	0.25
Ripple factor of V_o (K_C)	0.005
Switching frequency (f_{sw})	100 kHz

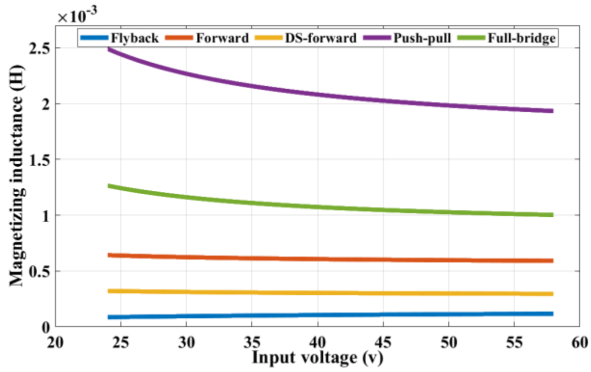

Fig. 3. Magnetizing inductance in the input voltage range of 24 to 58 V.

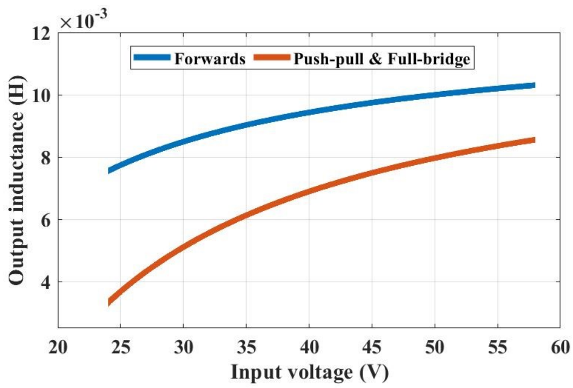

Fig. 4. Output inductance in the input voltage range of 24 to 58 V.

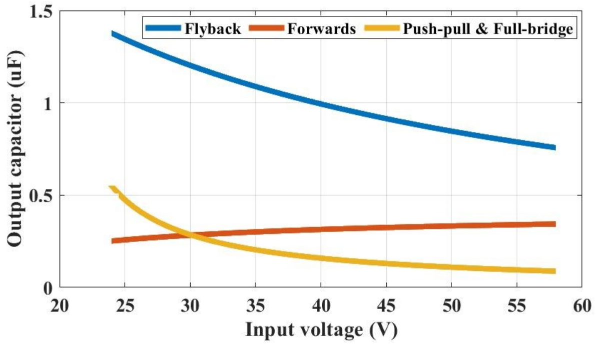

Fig. 5. Output capacitor in the input voltage range of 24 to 58 V.

B. Energy and sizing

In this section, the aim is to calculate the capacitive and inductive energy of the passive elements in the converters. Since the size of passive elements is determined using their energy, the energy consumed in the capacitor(s) and inductor(s) in these converters will be calculated for each of these converters. According to the design of converters and calculating the values of passive elements and then current and voltage of the circuit, inductor and capacitor energy can be obtained from the well-known energy equations. Fig. 6 shows the energy of the passive elements of each converter. In this figure, the calculated energy is normalized to maximum energy. As can be seen, the flyback converter needs the most energy in its passive elements. Therefore, in this converter, passive elements should have a larger size. Of course, the structure of the flyback magnetics core is different and there is an air gap in its core structure, working based on the coupling inductors. For the other four converters, the total energy value of the passive elements is much lower. Although push-pull and full-bridge converters have slightly higher total energy due to the larger output capacitor.

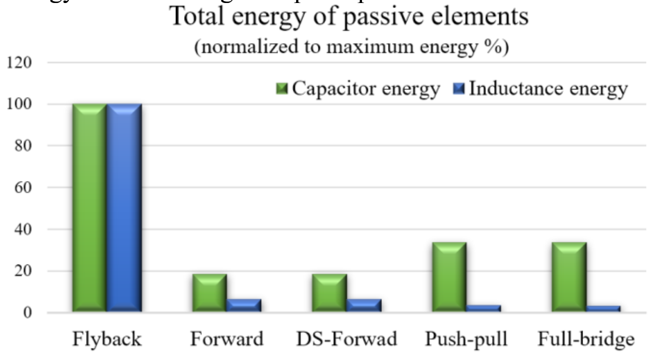

Fig. 6. The normalized total energy of passive elements in the converters

C. Selection of semiconductors

In selecting the semiconductor components of the converters, to select the appropriate switch and diode, their tolerable voltage and current must be calculated according to the specifications of the converter. The relationships between the maximum voltage and current of switches and diodes in different converters are given in Table I. The current passing through the switches and diodes can be easily calculated through the output load and the transformer conversion ratio. In this section, a comparison is made between the voltage across the switch and the output diode (D1) in the converters. As Fig. 7 shows, as the input voltage increases, the maximum voltage across the switch increases for all converters. Based on the equations in Table I, in DS-forward and full-bridge, the voltage across switch is Vin and for forward and push-pull is 2Vin. For flyback converter, this voltage is in range of Vin to 2Vin and based on its equation.

Fig. 8 also shows the maximum voltage across the output-side diode (D_1). In this figure also, the voltage across the output diode of all converters increases by increasing the input voltage. Based on equations in table and fixed output voltage and turn ratio, this voltage has been calculated. The lowest voltage across the diode is related to the full-bridge converter which is equal to nV_{in} and n in the full-bridge is 20. For a push-pull converter, this voltage has the highest value of $2nV_{in}$. For forward converters this voltage is equal to nV_{in} and to reach desirable output voltage, the turn ratio in forward converters was selected to be 38. Finally, for flyback, the voltage across diode is based on its equation in table I and is shown in Fig. 8.

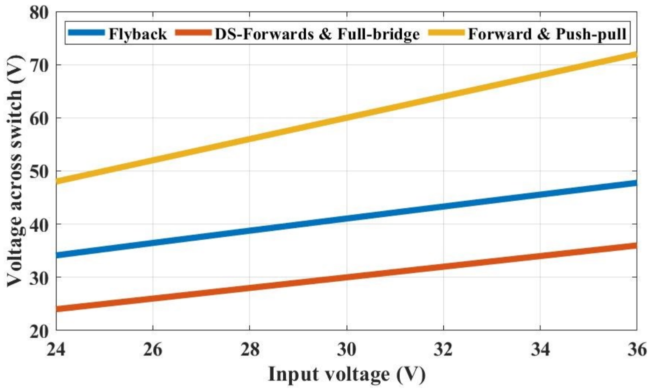

Fig. 7. The voltage across the switches in the converters.

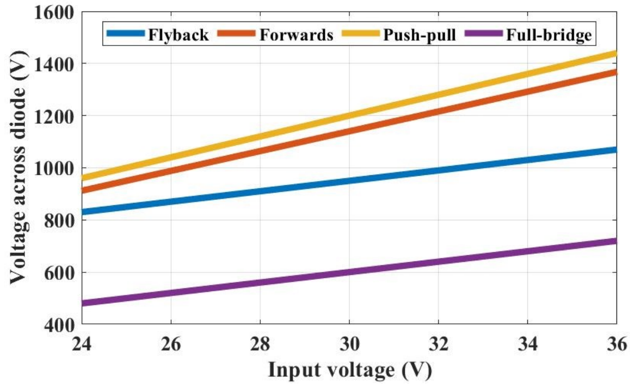

Fig. 8. The voltage across the secondary side diodes in the converters.

D. Losses

A comparison has also been made to investigate the semiconductor losses of these converters. In this comparison, switching and conduction losses of switches and conduction losses and forward voltage drop losses of diodes are considered. Due to the different numbers as well as the current and voltage of switches and diodes, their losses in each converter are calculated and compared. To calculate the losses, the conduction resistance value of the $R_{ds\text{-}on}$ switch is considered 0.008 Ohms, and the conduction resistance value of the diode is 0.004 Ohms. The average turn-on/off time of the switches is also assumed to be 100 ns for calculating switching losses. There is also a voltage drop across each diode of 0.4 V. With these assumptions and a switching frequency of 100kHz, Fig. 9 and 10 show a comparison between losses in different converters for two cases of input voltage. The values of these losses for each section are indicated in the figure.

As can be seen, the major amount of these losses is related to switching losses. By comparing the losses at 24 and 36 V input voltages, it can be concluded that at constant output load, at 24 V input voltage, due to the lower voltage across the switches, the switching losses are less than that of 36 V input voltage for all converters. Due to the constant output power, at 24 V input voltage, the input current (initial side of the transformer) will be higher and this will lead to more conduction losses than 36 V input voltage. As can be seen in Fig. 9 and 10, the highest losses are related to the switching losses of the forward converters, which is due to the higher current of switches. Although there is only one switch in forward converters, due to the higher voltage across the switch in this converters, switching losses are high. Also, as can be seen, in the DS-forward converter, the losses of two diodes in the primary side of the transformer that passes a high current

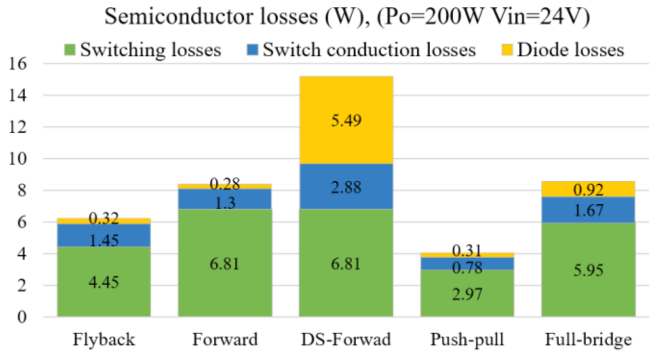

Fig. 9. Losses in semiconductor devices of the converters in V_{in}=24 V.

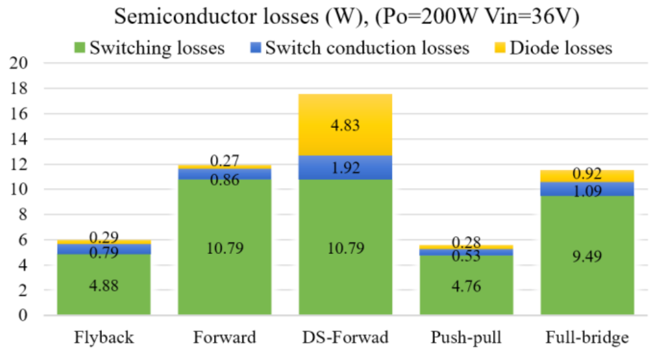

Fig. 10. Losses in semiconductor devices of the converters in V_{in}=36 V.

will lead to relatively high losses. In the push-pull converter, switching and conduction losses are reduced due to the input current being divided between the two paths. In the case of flyback and forward converters, it should be added that the switching losses for these two converters are calculated assuming the presence of snubber circuits that prevent voltage spikes. Of course, these snubber circuits also cause losses, which has a significant impact on the overall efficiency of the converter.

IV. Overall Comparison and Discussion

In this study, the general equations of five isolated dc-dc converters were extracted and then evaluated for a high step-up low-power application. According to the results, it can be said that the flyback converter has a simpler performance and fewer elements compared to other converters. However, with a high magnetizing current and high energy in the inductance of the magnetic core, this converter requires high consideration, including the air gap in the magnetic core. The other problem is related to the hard switching and voltage spike which need snubber circuits and this will result in additional losses.

The need for three windings in the single-switch forward converter and the high blocking voltage across the switch in this converter has reduced its popularity. Like a flyback converter, this converter also needs snubber circuits to alleviate voltage spikes. Although these problems have been fixed in the DS-forward converter, the presence of two switches and two diodes on the primary side increases the losses. In forward converters, the duty cycle limit is another factor to consider. In high gain applications, the duty cycle limitation in these converters must be overcome by increasing the transformer turn ratio, which in turn increases the size and cost, and on the other hand, also increases the maximum input current. As a result, a switch with a higher current rating will be needed. Given the above, push-pull and full-bridge converters seem to be better options. The advantages of these converters are the absence of limitations in the duty cycle

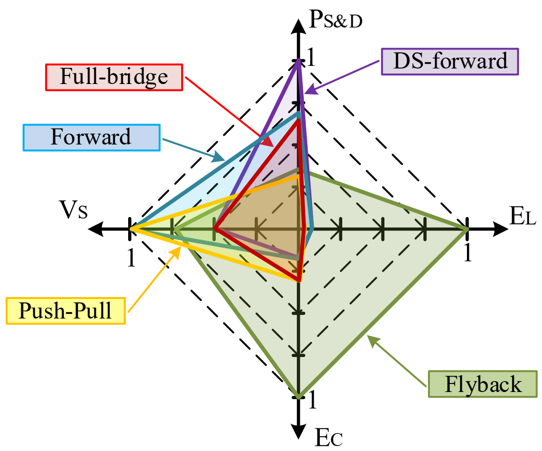

Fig. 11. Spider diagrams for an overall comparison between five desired converters in V_{in}=36 V.

and the reduction of the maximum input current. Also, there is no need for axillary circuits. In the push-pull converter, the presence of two switches with a lower current on the primary side will be associated with a reduction in losses. However, the need for a three tabs transformer in this converter can also be one of its disadvantages.

In the full-bridge converter, none of the above-mentioned problems exist for this converter. The only factor that can be a problem in this converter is the need for a large number of switches and diodes. This will result in losses and increase the size and cost to some extent. However, the cost is approximately equal to the cost of switch/diode(s) and snubber circuits in flyback and forward converters.

For an overall comparison and a better understanding of the above, an illustrative scheme is used in Fig. 11. In this diagram, four factors of switch and diode losses ($P_{S\&D}$), inductive energy (E_L), capacitive energy (E_C) and switch voltage stress (V_S), have been investigated. The values of these factors are normalized to the maximum value in these converters. It should be noted that this diagram is drawn for input voltage of 36 V. In the case of 24 V input voltage, the results are almost the same and there is only a slight difference in the amount of switch losses. This diagram introduces push-pull and full-bridge converters as relatively superior choices. Although the smaller area in this diagram indicates the overall better performance of the converter, the importance of each of these factors should be considered separately in order to make the best choice. For instance, in some applications, losses may be more important than converter size/weight or vice versa.

V. Conclusion

In this study, five isolated converters for a high step-up low-power application were evaluated from different aspects. After examination, it was found that the flyback converter requires a larger capacitor/magnetics and more considerations are required in its coupled inductors design. In terms of losses, with increasing input voltage, switching losses increase and conduction losses decrease at constant output power. The main losses in these converters were related to switching losses, and DS-forward converter had higher losses due to the high current of switches. Push-pull converter with a simpler structure had less losses. For forward converter that only have one switch, switching losses were relatively high due to the high voltage across the switch. Also, in the DS-forward, due to the presence of two diodes on the primary side, the diode losses were relatively high.

VI. Acknowledgment

This project has received funding from the European Union's Framework Programme for Research and Innovation Horizon 2020 (2014-2020) under the Marie Skłodowska-Curie Grant Agreement No955614.

VII. References

[1] M. Azizi, O. Husev, and D. Vinnikov, "Single-Stage Buck–Boost Inverters: A State-of-the-Art Survey," Energies, vol. 15, no. 5, p. 1622, Feb. 2022.

[2] O. Husev, O. Matiushkin, D. Vinnikov, C. Roncero-Clemente and S. Kouro, "Novel Concept of Solar Converter With Universal Applicability for DC and AC Microgrids," in IEEE Transactions on Industrial Electronics, vol. 69, no. 5, pp. 4329-4341, May 2022.

[3] V. Ravi and N. Lakshminarasamma, "Modeling, Analysis, and Implementation of High Voltage Low Power Flyback Converter Feeding Resistive Loads," in IEEE Transactions on Industry Applications, vol. 54, no. 5, pp. 4682-4695, Sept.-Oct. 2018.

[4] R. Hasan, W. Hassan and W. Xiao, "A High Gain Flyback DC-DC Converter for PV Applications," 2020 IEEE REGION 10 CONFERENCE (TENCON), 2020, pp. 522-526.

[5] Hasan, Rasedul, Waqas Hassan, Majid Farhangi, Saad Mekhilef, and Weidong Xiao. "Enhanced soft - switching strategy for flyback - based microinverter in PV power systems." IET Renewable Power Generation 13, no. 15 (2019): 2830-2839.

[6] Hong, Sung-Soo, Sang-Keun Ji, Young-Jin Jung, and Chung-Wook Roh. "Analysis and design of a high voltage flyback converter with resonant elements." Journal of Power Electronics 10, no. 2 (2010): 107-114.

[7] M. A. Rezaei, K. -J. Lee and A. Q. Huang, "A High-Efficiency Flyback Micro-inverter With a New Adaptive Snubber for Photovoltaic Applications," in IEEE Transactions on Power Electronics, vol. 31, no. 1, pp. 318-327, Jan. 2016.

[8] N. Sukesh, M. Pahlevaninezhad and P. K. Jain, "Analysis and Implementation of a Single-Stage Flyback PV Microinverter With Soft Switching," in IEEE Transactions on Industrial Electronics, vol. 61, no. 4, pp. 1819-1833, April 2014.

[9] S. Zengin, F. Deveci and M. Boztepe, "Decoupling Capacitor Selection in DCM Flyback PV Microinverters Considering Harmonic Distortion," in IEEE Transactions on Power Electronics, vol. 28, no. 2, pp. 816-825, Feb. 2013.

[10] Erickson, Robert W., and Dragan Maksimovic. Fundamentals of power electronics. Springer Science & Business Media, 2007.

[11] Instruments, Texas. "200-W interleaved forward converter design review using TI's UCC28221 PWM controller', TI." Inc., Application Notes (2004).

[12] H. Tarzamni, E. Babaei, F. P. Esmaeelnia, P. Dehghanian, S. Tohidi and M. B. B. Sharifian, "Analysis and Reliability Evaluation of a High Step-Up Soft Switching Push–Pull DC–DC Converter," in IEEE Transactions on Reliability, vol. 69, no. 4, pp. 1376-1386, Dec. 2020.

[13] B. Zhao, Q. Song, W. Liu and Y. Sun, "Overview of Dual-Active-Bridge Isolated Bidirectional DC–DC Converter for High-Frequency-Link Power-Conversion System," in *IEEE Transactions on Power Electronics*, vol. 29, no. 8, pp. 4091-4106, Aug. 2014.

[14] G. E. Sfakianakis, J. Everts, H. Huisman and E. A. Lomonova, "Comparative Evaluation of Bidirectional Dual Active Bridge DC-DC Converter Variants," 2016 IEEE Vehicle Power and Propulsion Conference (VPPC), 2016, pp. 1-6.

[15] A. Y. N and A. N. Nagashree, "Analytical comparision of Dual Active Bridge converter with Push Pull Converter for power transfer efficiency," 2019 Global Conference for Advancement in Technology (GCAT), 2019, pp. 1-4.

[16] Bai H, Mi C. Comparison and evaluation of different DC/DC topologies for plug-in hybrid electric vehicle chargers. International Journal of Power Electronics. 2012 Jan 1;4(2):119-33.

[17] N. M. L. Tan, T. Abe and H. Akagi, "Topology and application of bidirectional isolated dc-dc converters," 8th International Conference on Power Electronics - ECCE Asia, 2011, pp. 1039-10.

.